Chem. Chem. Technol., 2026,
Vol. 20, No. 1, pp. 118–125

Chemistry

OXYGEN ELECTROREDUCTION ON SILVER / COPPER NANOSTRUCTURED CATHODES

Vasyl Skrypnychuk[1,✉], Galyna Zozula[1], Vasyl Kordan[2], Orest Kuntyi[1]

[1] Lviv Polytechnic National University, 12, S. Bandery str., Lviv, 79013, Ukraine
[2] Ivan Franko National University of Lviv, 6, Kyryla i Mefodiya str., Lviv, 79005, Ukraine
✉ *skrypnychuk@gmail.com*

https://doi.org/10.23939/chcht20.01.118

Abstract. We report the fabrication of catalytically active AgNPs/Cu oxygen reduction cathodes using the method of galvanic replacement of copper with silver in $K[Ag(CN)_2]$ solutions. It was shown that the formed AgNPs with an average size < 50 nm are uniformly distributed on the copper surface, and their content depends on the concentration of the cyanocomplex and the duration of the GR process. It was determined that in a broad silver concentration range (0.02–0.86 at. %) on the copper surface, the AgNPs/Cu cathodes exhibit 15 % higher ORR activity than silver cathodes, and exhibit superior parameters E_{onset} (by ~0.02 V) and $E_{1/2}$ (by ~0.05 V). The testing results in alkaline zinc-air fuel cells showed that the discharge voltage of cells based on AgNPs/Cu cathodes rivals that of the cells based on silver cathodes.

Keywords: ORR, bimetallic surface, AgNPs/Cu cathode, galvanic replacement, $K[Ag(CN)_2]$ solutions.

1. Introduction

Low activity of oxygen reduction reaction (ORR) remains one of the main factors that limit the practical application of promising electricity sources – fuel cells[1,2] and secondary metal-air batteries.[3–5] ORR is a catalytic process and nowadays the insufficient efficiency of existing electrocatalysts of the oxygen reduction reaction remains a problematic issue considering the cost – activity – durability – scalability relationship. The most active and the most well studied catalysts are based on platinum.[6–8] However, the high cost of platinum and the limited natural abundance of this metal do not allow to provide scalability for power source manufacturing. Hence, over the last decade, we have observed an active search for inexpensive platinum-free catalysts with high catalytic activity of the oxygen reduction reaction.[9] Among the metals alternative to platinum, one should mention cathodes based on silver,[10] which is inferior only to platinum and palladium in terms of O_2 bonding energy and its intermediate products with Ag atoms.[11] This property is one of the main ORR efficiency criteria. Considering the fact that silver is dozens of times cheaper than platinum and its natural reserves are much higher, silver[12–16] and silver-containing[17–27] materials are considered to be promising catalytically active oxygen reduction cathodes, which is supported by the publication activity of recent years. A lot of emphasis has been placed on the nanoscale effect, using nanoparticles and nanostructured electrode surfaces.

Among silver-containing cathodes binary systems deserve special attention, in particular nanoalloys AgM[18–24] and bimetals Ag/M,[25–27] where M – metal that causes synergism between metallic components Ag and M. Authors[17] explain this effect by three different reasons: 1) geometric (or strain) effect, which is caused by lattice distortion by the second metal (M); 2) electronic (or ligand) effect of the second metal (M), which alters the electronic configuration of the active metal site and therefore enhances its catalytic activity; 3) stabilizing effect, which manifests itself by supporting of the catalytic activity (preventing poisoning) by the second metal (M) during the prolonged ORR process.

Ag/Cu is one of the bimetallic nanostructured systems for catalytically active cathodes, where the synergistic effect of ORR is revealed.[25–27] Low cost and scalability of the second metal (copper) make such a system very promising. One of the most promising approaches in this direction is the formation of silver nanostructures on a copper substrate to provide the nanoscale effect. The use of a metal substrate is also relevant as an alternative to highly active electrode substrates based on carbon nanomaterials. According to research results over the past decade, the latter are harmful to living organisms in the natural environment and are difficult to degrade under natural conditions.[28]

The purpose of the research is the determination of the ORR electrocatalytic activity of the AgNPs/Cu bimetallic system synthesized by galvanic replacement (GR) of silver on copper substrate in the solution of $[Ag(CN)_2]^-$ complex.

2. Experimental

2.1. Materials

All chemicals were analytical grade reagents and used as received without further purification. A 1 mm-thick copper sheet (99.9 wt. % Cu) was used as a copper deposition substrate. For the latter, $CuSO_4 \cdot 5H_2O$ (99.9 mass. %, Aldrich) and 96.5 % solution of H_2SO_4 were used. For the modification of the copper-coated surface with silver, a complex salt, $K[Ag(CN)_2]$ (99.99 %, Aldrich), was used. Electrochemical oxygen reduction reaction was carried out using 0.1M aqueous solutions of KOH (99.9 %, Aldrich) in distilled water. Cleaning of the substrates was done in ethanol (96 %). Graphite plate anodes were used as counter-electrodes, and a silver / silver chloride electrode (Ag/AgCl) was applied as a reference electrode.

2.2. Methods

2.2.1. Preparation of electrodes

Copper plates were cleaned in ethanol and etched in the mixture of sulphuric and nitric acid (3:1), followed by washing with distilled water. Before the modification of the copper substrate with silver nanoparticles, the copper plates were plated with copper, which ensured high purity and topographical uniformity of the surface, hence uniform conditions of the process of galvanic replacement. The deposition of electrolytic copper was performed in an acidic sulfate bath (150 $g \cdot L^{-1}$ $CuSO_4 \cdot 5H_2O$, 50 $g \cdot L^{-1}$ H_2SO_4) at 20 °C and a current density of 1 $A \cdot dm^{-2}$ for 30 min. After copper deposition, the plates were washed sequentially with distilled water and ethanol in an ultrasound bath (Jeken Codyson CD-4800, 70 W output and 42 kHz) for 30 s and dried in air at 60 °C. The copper-coated plate was cut into samples of 1×1 cm, which were further used for silver modification.

Deposition of silver onto the copper surface was performed by galvanic replacement from 0.1–50 mM solutions of $K[Ag(CN)_2]$ during 5–300 s. The modification process was performed in a thermostated glass vessel with a solution volume of 50 cm^3 in an ultrasonic field at a temperature of 20 °C. After the deposition of AgNPs on the surface of copper the samples were sequentially washed in distilled water and ethanol in the ultrasonic bath for 30 s and dried in air at 60 °C.

2.2.2. Cathodic reduction of O_2 on the surface of silver-modified copper

Electrochemical reduction of O_2 on the silver-modified copper cathodes was studied using the methods of cyclic voltammetry and chronoamperometry in 0.1 M KOH. Prior to measurement, the solution was saturated with oxygen for 30 min. The study was performed in a standard three-electrode electrochemical cell with a volume of 200 mL. The cell was equipped with a silver-modified copper (AgNPs/Cu) 1×1 cm working electrode, an auxiliary graphite plate electrode, and a saturated silver-silver chloride reference electrode (Fig. 1). Cyclic voltammograms for the copper electrode were measured in the potential range E = –0.1–(–0.6) V *vs.* Ag/AgCl using a scan rate of 50 $mV \cdot s^{-1}$, and potentiostatic electrolysis was done at E = –0.325 V. Electrochemical studies were performed using the VersaSTAT 4-500 potentiostat-galvanostat.

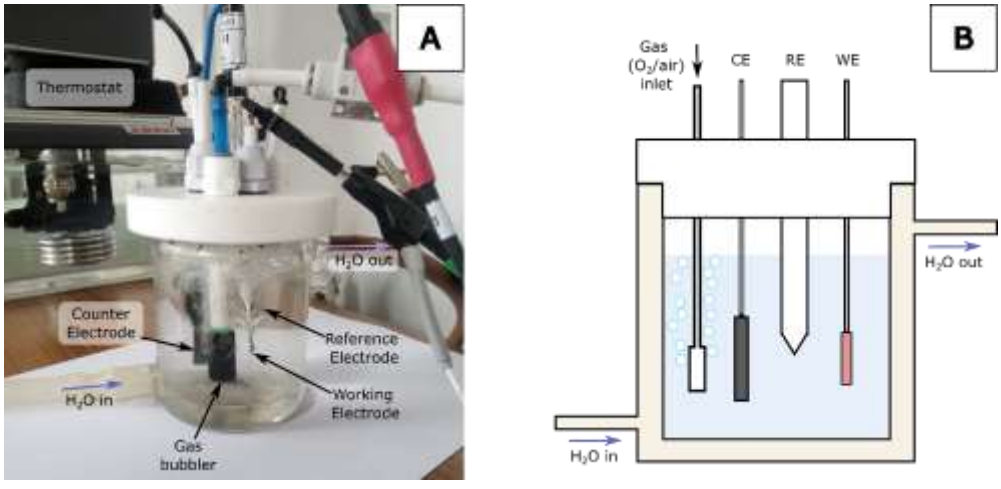

Fig. 1. Photograph (A) and diagram (B) of the electrochemical cell used for ORR studies

The ORR cathodes were used as electrodes in model zinc-air fuel cells in flow configuration (Fig. 2). This fuel cell setup comprised two flat electrodes, namely a zinc foil anode and an ORR cathode, which was being tested. These electrodes were attached to graphite foil current collectors and enclosed between acrylic plastic sheets, ensuring that the interelectrode distance was 4 mm. Silicone sheets were used as sealing components, and the cell stack was pressed together by steel threaded bolts (not shown in the diagram). The active area of the electrodes was 1×1 cm. Solution of electrolyte (1 M KOH) was circulated between these two electrode plates using a circulation pump (Seko Invicta KCS632, flow rate 2 l h^{-1}) equipped with a damper in order to provide an uniform electrolyte flow rate. The electrolyte was constantly purged with air using an air pump (SunSun CT-202) and homogenised using a magnetic stirrer.

Electrochemical fuel cell discharge tests were performed using 5 min OCV measurement step followed by 5 min discharge step at a specified current density. The discharge current density was gradually increased from 0.5 mA cm^{-2} to 3 mA cm^{-2} with a step of 0.5 mA cm^{-2}. Fuel cell testing was performed using the BTS4000 battery tester (Neware).

2.2.3. Morphological study

SEM examination of the samples was carried out by using electron microscope Tescan Vega 3 LMU equipped with an X-MaxN 20 silicon drift detector. Overall compositions were investigated using energy-dispersive X-ray spectroscopy (EDX); Gun voltage 25 kV, imaging mode with SE and BSE detectors, working distance 15–16 mm, vacuum 10^{-3} Pa.

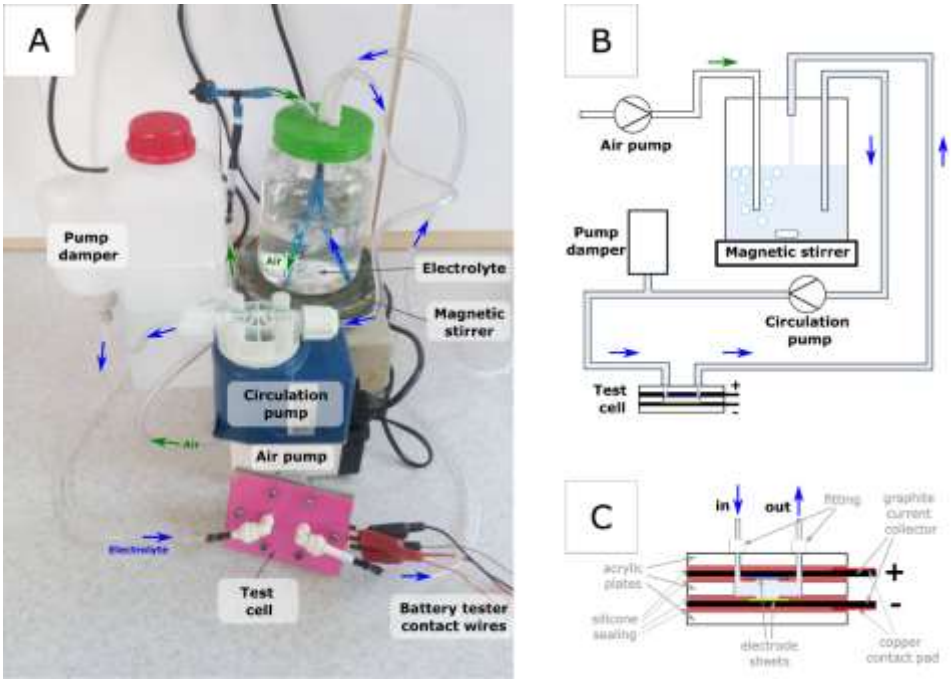

Fig. 2. Photograph (A) and diagram (B) of the electrochemical setup used for zinc-air fuel cell discharging experiments. (C) Detailed diagram of the components of the zinc-air test cell

3. Results and Discussion

3.1. Formation of AgNPs/Cu on copper surface by galvanic replacement in $[Ag(CN)_2]^-$ solution

Silver nanoparticles with dimensions ≤50 nm can be deposited on a copper surface in a wide range of $K[Ag(CN)_2]$ concentrations (0.1–50 mM) and galvanic replacement time (5–300 s). A typical example is shown in Fig. 3A. At the same time, the size of AgNPs and their distribution are practically identical at the edges, faces and vertices of the sub-micron copper crystals. The distribution uniformity of the nanoparticles is observed over the whole surface of the substrate (Fig. 3B). It is caused by the peculiarity of the process of galvanic displacement in solutions of cyanide complex $[Ag(CN)_2]^-$, which can be represented by the overall equation of the reaction (1). High stability of $[Ag(CN)_2]^-$ (K = $1 \cdot 10^{-21}$)

causes a significant shift of the electrode potential towards negative values compared to the hydrated ion ($E^0_{Ag(CN)_2^-/Ag}$ = –0.30 V, $E^0_{Ag^+/Ag}$ = 0.799 V). This property provides high polarization, which favors the formation of nanostructures during the reduction of silver on cathodic areas (2) and its uniform distribution on the sacrificial surface.[29] Besides, in solutions of stable complexes, the process of galvanic replacement occurs either according to the Vollmer – Weber mechanism with the formation of island precipitate on the substrate or according to the Frank-van der Merwe mechanism with the formation of a porous layer.[30] At the anodic areas, the dissolution of the sacrificial copper occurs, leading to the formation of the soluble cyanocomplex $[Cu(CN)_2]^-$ (3).

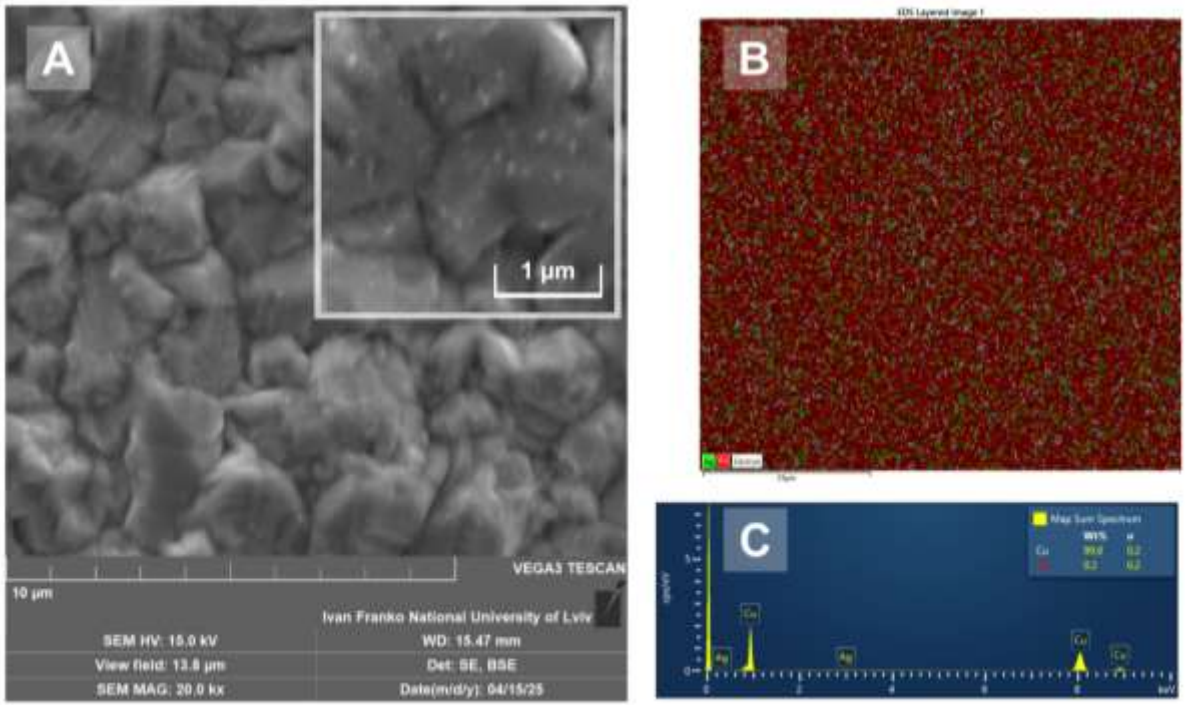

Fig. 3. (A) SEM image, (B) EDS map, and (C) EDS spectrum of Ag/Cu surface after silver deposition on copper by galvanic replacement in 10 mM $K[Ag(CN)_2]$ for 15 s

$$Cu + [Ag(CN)_2]^- \rightarrow [Cu(CN)_2]^- + Ag \quad (1)$$

at cathodic areas (–): $[Ag(CN)_2]^- + e \rightarrow Ag + 2CN^-$ (2)

at anodic areas (+): $Cu + 2CN^- \rightarrow [Cu(CN)_2]^- + e$ (3)

The process of galvanic replacement occurs according to the electrochemical mechanism, and its rate primarily depends on the electromotive force (ΔE^0), which is a function of the difference between the standard electrode potentials of the metal being reduced and the sacrificial metal.[30] For the reaction (1) ΔE^0 is small (4), therefore the main parameters of the silver reduction rate at the copper surface are $[Ag(CN)_2]^-$ ions concentration and process duration. The latter indirectly affects the silver content at the surface of the copper substrate, which is primarily caused by the slowing down of the rate of the electron-generating reaction (3) due to the decrease of the active surface area of the sacrificial metal (copper). However, the trend of dependence of silver content on $K[Ag(CN)_2]$ concentration and GR duration is observed (see Table 1).

$$\Delta E^0 = E^0_{Ag(CN)_2^-/Ag} - E^0_{Cu(CN)_2^-/Cu} = \\ = -0.30 - (-0.43) = 0.13 \text{ V} \quad (4)$$

Table 1. Surface silver content based on EDX data

Parameters	Sample *N*				
	1	2	3	4	5
$K[Ag(CN)_2]$ concentration, mmol·l^{-1}	1	10	10	10	50
Duration, s	15	5	15	60	300
Surface silver content, at. %	0.08	0.02	0.12	0.17	0.86

3.2. Oxygen reduction reaction on AgNPs/Cu cathodes

Molecular oxygen bonding energy and, respectively, the catalytic activity of the copper cathode in oxygen reduction are significantly inferior to that of the silver cathode.[11] Hence, it is expected that the O_2 reduction current values on the silver plate will be significantly higher than such values on the copper plate (Fig. 4A). The maximal values of cathodic current density ($i_{cathode}$) on nanostructured AgNPs/Cu cathodes exceed the values of this quantity compared to the silver cathode only by ~15 %. However, they differ fundamentally by the character of the I–V curves and by the important characteristics of the ORR process, namely the onset potential of the diffusion-limited region of oxygen reduction and the value of half of its wave (Fig. 4). For the AgNPs/Cu cathodes, in a wide silver content range, the maximum of cathodic current of the ORR process is observed at about –0.3 V, which is 0.15–0.2 V earlier compared to silver.

The values of E_{onset} and $E_{1/2}$ are observed earlier too, by ~0.02 V and ~0.05 V, respectively. Apart from the nanoscale effect, such a significant enhancement of the main ORR parameters is caused by the mutual effect of both metals at the nanostructure level. Cu and Ag have identical electronic configurations, so the enhancement of the catalytic activity of silver due to the electronic effect of the second metal (Cu) is not observed. Such an effect is characteristic of metals, the atoms of which contain unoccupied *d*-orbitals, for example, in group 8 *d*-block metals, which cause the electronic effect in bimetals AgCo,[19] AgFe,[31] AgPd.[32] Hence, the effect of the 'second metal' here can be explained by the geometric effect, which is caused by lattice distortion due to the second metal (Cu). Since Cu and Ag have identical crystalline lattice (cubic face-centered), and the difference between their atomic radii is smaller than 15 %, which favors the formation of substitutional solid solutions. As shown in the study,[33] random substitutions of Cu atoms with Ag atoms cause the alteration of the crystalline lattice parameters of silver, which in turn leads to its thermodynamic instability and hence the increase of catalytic activity.

Temporal stability of the catalytic activity of the oxygen reduction process on nanostructured AgNPs/Cu cathodes increases with the increase of silver content at its surface (Fig. 5). For the sample with surface silver content of 0.17 at. % (sample 4), $i_{cathode}$ after 60 min of the ORR process was 20–30 % higher than such a value for the cathode containing 0.08 at. % silver (sample 1). This difference may be related to the partial oxidation of the copper surface.

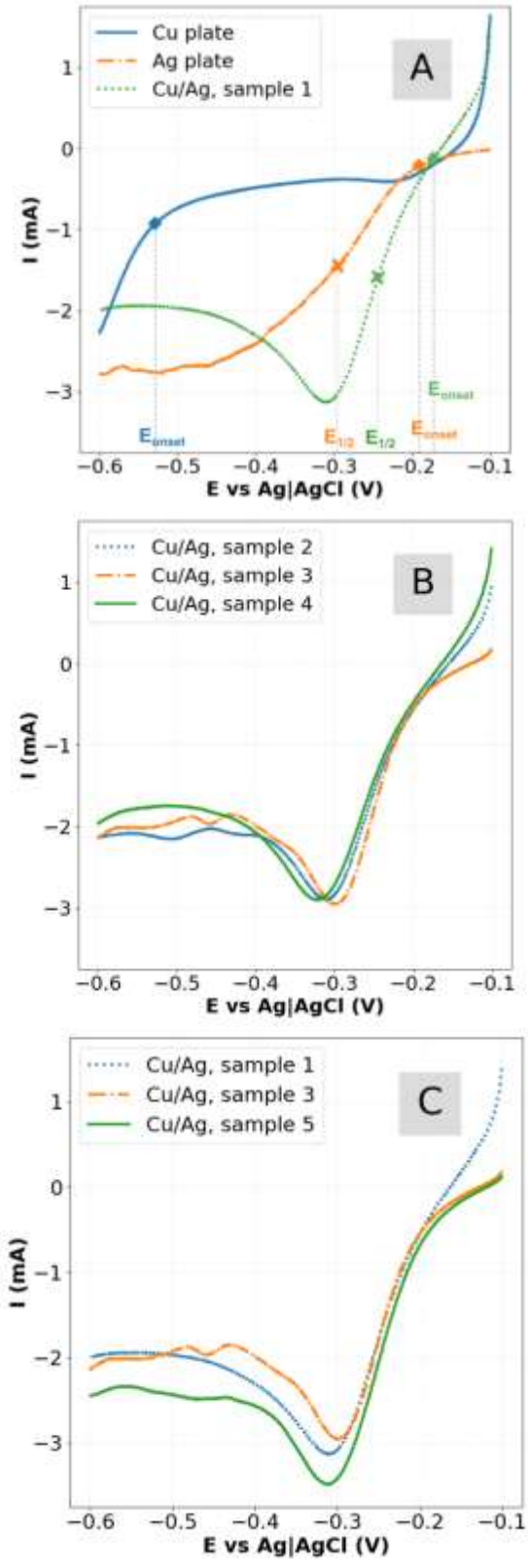

Fig. 4. Voltammetry curves for ORR measurements, scan rate 50 mV·s^{-1}

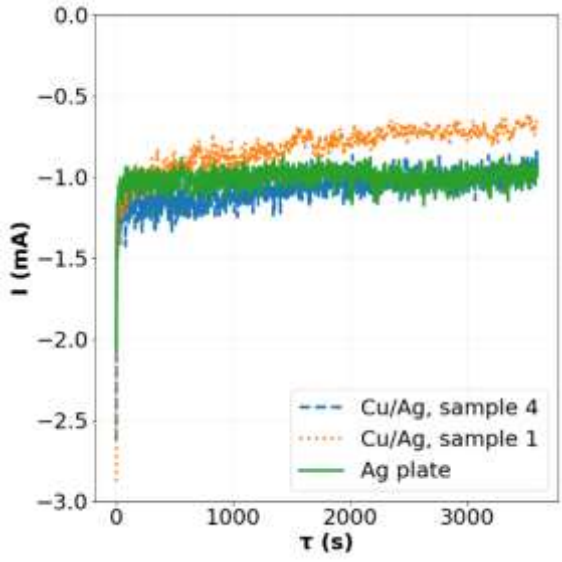

Fig. 5. Chronoamperometry data for the ORR process on nanostructured AgNPs/Cu cathodes measured at the potential of -0.325 V *vs.* Ag/AgCl

The character of the CV curve for ORR process using air-saturated ORR is identical to the curve obtained using pure oxygen (Fig. 6). The $i_{cathode}$ values are 2–3 times smaller than the corresponding values obtained using pure oxygen. It exceeds the expected value, considering the oxygen content in the air of ~20 %.

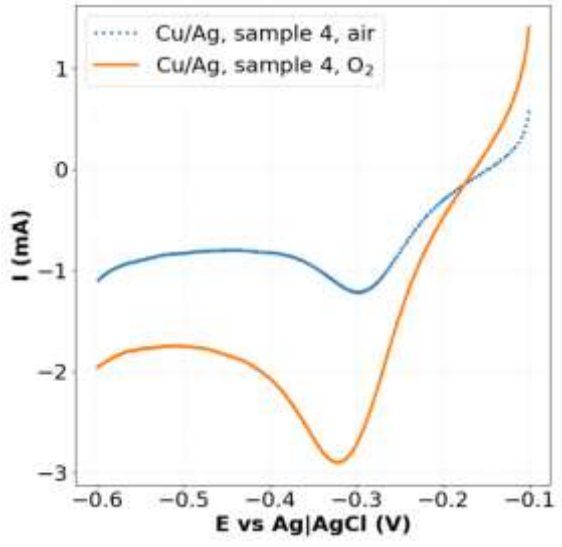

Fig. 6. Voltammetry curves for ORR measurements using air (dotted blue line) and pure oxygen (solid orange line), scan rate 50 mV s^{-1}

The ORR performance of both silver plate cathodes and Cu/Ag foil cathodes was tested in alkaline zinc-air fuel cells using flowing air-saturated 1M KOH electrolyte, *i. e.*, without fabrication of the dedicated gas diffusion electrode. In terms of ORR electrode operation, this configuration is directly equivalent to the three-electrode testing configuration discussed above.

As shown in Fig. 7, the discharge voltage of zinc-air fuel cells based on Cu/Ag cathodes rivals the voltage values of the cells base on pristine Ag plate cathodes for all the discharge voltages (0.5–3 mA cm^{-2}) used.

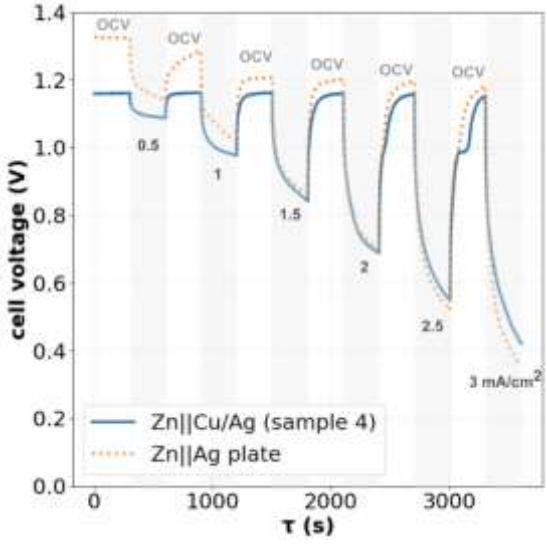

Fig. 7. Zinc-air fuel cell testing data using zinc foil anodes and silver plate (dotted orange line) or Cu/Ag foil (solid blue line) cathodes

4. Conclusions

Widespread application of highly efficient platinum catalytic oxygen reduction cathodes in metal-air fuel cells is limited by the high cost of this rare metal. Therefore, one of the alternatives is nanostructured silver and silver-containing ORR cathodes and primarily bimetallic AgM. Among the latter, systems AgNPs/Cu are promising in terms of cost-efficiency ratio.

Using galvanic replacement of silver on copper substrate in solutions of $K[Ag(CN)_2]$, we ensure the formation of catalytically active AgNPs/Cu cathodes with uniform distribution of AgNPs with dimensions of <50 nm. The silver content on the surface of the substrate is regulated by two main parameters – concentration of the silver cyanocomplex and duration of the GR process.

In a broad range of AgNPs content (0.02–0.86 at. %) catalytic activity of the AgNPs/Cu oxygen reduction cathodes is high. Manifestations of nanoscale effect caused by the size of AgNPs and geometric effect

caused by lattice distortion due to the second metal (Cu) lead to the enhancement of such electrochemical ORR parameters compared to the silver cathode: increase of cathode currents by 15 %, the cathode current maximum of the process appears 0.15–0.2 V earlier compared to silver, the values of E_{onset} and $E_{1/2}$ values appear earlier by ~0.02 V and ~0.05 V respectively.

The obtained AgNPS/Cu cathodes exhibit similar properties to silver cathodes when tested in alkaline zinc-air fuel cells. Considering that the silver contents at the surface of AgNPs/Cu are two orders of magnitude smaller than in pure silver cathodes, the obtained nanostructured bimetallic AgCu cathodes are promising for metal-air fuel cell applications.

Acknowledgements

This work was carried out with the partial financial support of the National Research Foundation of Ukraine. Project registration number: 2025.07/0068 ("Bimetallic nanostructures formed via laser treatment and decoration of 3D substrates by galvanic replacement in electro-chemical catalysis: design, architecture of electrodes, topography, activity, stability").

References

[1] Qasem, N. A. A.; Abdulrahman, G. A. Q. A Recent Comprehensive Review of Fuel Cells: History, Types, and Applications. *Int. J. Energy Res.* **2024**, *2024*, 7271748. https://doi.org/10.1155/2024/7271748

[2] Li, S.; Ho, S.-H.; Hua, T.; Zhou, Q.; Li, F.; Tang, J. Sustainable Biochar as an Electrocatalysts for the Oxygen Reduction Reaction in Microbial Fuel Cells. *Green Energy Environ.* **2021**, *6*, 644–659. https://doi.org/10.1016/j.gee.2020.11.010

[3] Salado, M.; Lizundia, E. Advances, Challenges, and Environmental Impacts in Metaleair Battery Electrolytes. *Mater. Today Energy* **2022**, *28*, 101064. https://doi.org/10.1016/j.mtener.2022.101064

[4] Lv, X.-W.; Wang, Z.; Lai, Z.; Liu, Y.; Ma, T.; Geng, J.; Yuan, Z.-Y. Rechargeable Zinc–Air Batteries: Advances, Challenges, and Prospects. *Small* **2024**, *20*, 2306396. https://doi.org/10.1002/smll.202306396

[5] Jose, S. A.; Doering, E.; Klein, N.; Mena, E. I.; Owens, C.; Pronk S.; Menezes, P. L. Magnesium – Air Batteries: Manufacturing, Processing, Performance, and Applications. *Processes* **2025**, *13*, 607. https://doi.org/10.3390/pr13030607

[6] Hussain, S.; Erikson, H.; Kongi, N.; Sarapuu, A.; Solla-Gullon, J.; Maia, G.; Kannan, A. M.; Alonso-Vante, N.; Tammeveski, K. Oxygen Reduction Reaction on Nanostructured Pt-Based Electrocatalysts: A Review. *Int. J. Hydrog. Energy* **2020**, *45*, 31775–31797. https://doi.org/10.1016/j.ijhydene.2020.08.215

[7] Ali, A.; Laaksonen, A.; Huang, G.; Hussain, S.; Luo, S.; Che, W.; Shen, P. K.; Zhu, J.; Ji, X. Emerging Strategies and Developments in Oxygen Reduction Reaction Using High-Performance Platinum-Based Electrocatalysts. *Nano Res.* **2024**, 17, 3516–3532. https://doi.org/10.1007/s12274-023-6310-x

[8] Đukić, T.; Pavko, L.; Jovanovic, P.; Maselj, N.; Gatalo, M. Hodnik, N. Stability Challenges of Carbon-Supported Pt-Nanoalloys as Fuel Cell Oxygen Reduction Reaction Electrocatalysts. *ChemComm*. **2022**, *58*, 13832–13854. https://doi.org/10.1039/d2cc05377b

[9] Hao, Z.; Ma, Y.; Chen, Y.; Fu, P.; Wang, P. Non-Noble Metal Catalysts in Cathodic Oxygen Reduction Reaction of Proton Exchange Membrane Fuel Cells: Recent Advances. *Nanomaterials* **2022**, *12*, 3331. https://doi.org/10.3390/nano12193331

[10] Erikson, H.; Sarapuu, A.; Tammeveski, K. Oxygen Reduction Reaction on Silver Catalysts in Alkaline Media: a Minireview. *ChemElectroChem*. **2019**, *6*, 73–86. https://doi.org/10.1002/celc.201800913

[11] Nørskov, J. K.; Rossmeisl, J.; Logadottir, A.; Lindqvist, L.; Kitchin, J. R.; Bligaard, T.; Jónsson, H. Origin of the Overpotential for Oxygen Reduction at a Fuel-Cell Cathode. *J. Phys. Chem. B.* **2004**, *108*, 17886–17892. https://doi.org/10.1021/jp047349j

[12] Linge, J. M.; Erikson, H.; Kasikov, A.; Rähnb, M.; Sammelselg, V.; Tammeveski, K. Oxygen Reduction Reaction on Thin-Film Ag Electrodes in Alkaline Solution. *Electrochim. Acta* **2019**, *325*, 134922. https://doi.org/10.1016/j.electacta.2019.134922

[13] Ganesh, P. A.; Prakrthi, A. N.; Chandrasekaranc, S. S.; Jeyakumar, D. Shape-Tuned, Surface-Active and Support-Free Silver Oxygen Reduction Electrocatalyst Enabled High Performance Fully non-PGM Alkaline Fuel Cell. *RSC Adv.* **2021**, *11*, 24872–24882. https://doi.org/10.1039/d1ra02718b

[14] Linge, J. M.; Kozhemyakin, D.; Erikson, H.; Vlassov, S.; Kongi, N.; Tammeveski, K. Silver Nanowire-Based Catalysts for Oxygen Reduction Reaction in Alkaline Solution. *ChemCatChem*. **2021**, *13*, 4364–4371. https://doi.org/10.1002/cctc.202100758

[15] Arumugam, B.; Kuppuswamy, G. P.; Sivalingam, Y. Electrocatalytic Oxygen Reduction Reaction at Silver Nanoparticles (AgNPs) Electrode in Neutral Solution: 5-amino-2-naphthalene-sulfonic acid (ANS) as a Reducing Agent for AgNPs. *ECS J. Solid State Sci. Technol*. **2022**, *11*, 023010. https://doi.org/10.1149/2162-8777/ac4799

[16] Rampf, A.; Braig, M.; Passerini, S.; Zeis, R. A Comparative Study of the Oxygen Reduction Reaction on Pt and Ag in Alkaline Media. *ChemElectroChem*. **2025**, *12*, e202400563. https://doi.org/10.1002/celc.202400563

[17] Zhao, K.; Shu, Y.; Li, F.; Peng, G. Bimetallic Catalysts as Electrocatalytic Cathode Materials for the Oxygen Reduction Reaction in Microbial Fuel Cell: A Review. *Energy Environ.* **2023**, *8*, 1043–1070. https://doi.org/10.1016/j.gee.2022.10.007

[18] Dembinska, B.; Brzozowska, K.; Szwed, A.; Miecznikowski, K.; Negro, E.; Noto, V.; Kulesza, P. J. Electrocatalytic Oxygen Reduction in Alkaline Medium at Graphene-Supported Silver-Iron Carbon Nitride Sites Generated During Thermal Decomposition of Silver Hexacyanoferrate. *Electrocatalysis* **2019**, *10*, 112–124. https://doi.org/10.1007/s12678-018-0501-3

[19] Milikić, J.; Knežević, S.; Stojadinović, S.; Alsaiari, M.; Harraz, F. A.; Santos, D. M. F.; Šljukić, B. Facile Synthesis of Low-Cost Copper-Silver and Cobalt-Silver Alloy Nanoparticles on Reduced Graphene Oxide as Efficient Electrocatalysts for Oxygen Reduction Reaction in Alkaline Media. *Nanomaterials* **2022**, *12*, 2657. https://doi.org/10.3390/nano12152657

[20] Zeledón, J. A. Z.; Stevens, M. B.; Gunasooriya, G. T. K. K.; Gallo, A.; Landers, A. T.; Kreider, M. E.; Hahn, C.; Nørskov, J. K.; Jaramillo, T. F. Tuning the electronic structure of Ag-Pd alloys

to enhance performance for alkaline oxygen reduction. *Nature Commun*. **2021**, *12*, 620. https://doi.org/10.1038/s41467-021-20923-z
[21] Gibbons, B. M.; Wette, M.; Stevens, M. B.; Davis, R. C.; Siahrostami, S.; Kreider, M.; Mehta, A.; Higgins, D. C.; Clemens, B. M.; Jaramillo, T. F. In Situ X Ray Absorption Spectroscopy Disentangles the Roles of Copper and Silver in a Bimetallic Catalyst for the Oxygen Reduction Reaction. *Chem. Mater*. **2020**, *32*, 1819–1827. https://doi.org/10.1021/acs.chemmater.9b03963
[22] Yin, S.; Shen, Y.; Zhang, J.; Yin, H.-M.; Liu, X.-Z.; Ding, Y. Tuning the Electronic Structure of Nanoporous Ag *via* Alloying Effect from Cu to Boost the ORR and Zn-Air Battery Performance. *Appl. Surf. Sci*. **2021**, *545*, 149042. https://doi.org/10.1016/j.apsusc.2021.149042
[23] Chen, J.; Wang, Z.; Mao, J.; Liu, C.; Chen, Y.; Lu, Z.; Feng, S.-P. Bimetallic Ag-Cu Nanosheets Assembled Flower-Like Structure for Oxygen Reduction Reaction. *J. Alloys Compd*. **2021**, *856*, 157379. https://doi.org/10.1016/j.jallcom.2020.157379
[24] Zhang, N.; Chen, F.; Jin, Y.; Wang, J.; Jin, T.; Kou, B. Alloying Effect in Silver-Based Dilute Nanoalloy Catalysts for Oxygen Reduction Reactions. *J. Catal*. **2020**, *384*, 37–48. https://doi.org/10.1016/j.jcat.2020.02.009
[25] Lei, H.; Siwal, S. S.; Zhang, X.; Zhang, Q. Compositional and Morphological Engineering of in-situ-Grown Ag Nanoparticles on Cu Substrate for Enhancing Oxygen Reduction Reaction Activity: A Novel Electrochemical Redox Tuning Approach. *J. Colloid Interface Sci*. **2020**, *571*, 1–12. https://doi.org/10.1016/j.jcis.2020.03.020
[26] Thota, R.; Sundari, S.; Berchmans, S.; Ganesh, V. Silver – Copper Bimetallic Flexible Electrodes Prepared Using a Galvanic Replacement Reaction and Their Applications. *ChemistrySelect*. **2017**, *2*, 2114–2122. https://doi.org/10.1002/slct.201601810
[27] Beltrán-Gastélum, M.; Portillo-Fuentes, S.G.; Flores-Hernández, J. R.; Salazar-Gastélum, M. I.; Trujillo-Navarrete, B.; Romero-Castañón, T.; Silva-Carrillo, C.; Reynoso-Soto, E. A.; Félix-Navarro, R. M. Ag-Cu Nanoparticles as Cathodic Catalysts for an Anion Exchange Membrane Fuel Cell. *Catalysts* **2023**, *13*, 1050. https://doi.org/10.3390/catal13071050
[28] Peng, Z.; Liu, X.; Zhang, W.; Zengc, Z.; Liu, Z.; Zhang, C.; Liu, Y.; Shao, B.; Liang, Q.; Tang, W.; Yuan, X. Advances in the Application, Toxicity and Degradation of Carbon Nanomaterials in Environment: A Review. *Environ. Int*. **2020**, *134*, 10529. https://doi.org/10.1016/j.envint.2019.105298
[29] Kuntyi, O.; Shepida, M.; Sus, L.; Zozulia, H.; Korniy, S. Modification of Silicon Surface with Silver, Gold and Palladium Nanostructures via Galvanic Substitution in DMSO and DMF Solutions. *Chem. Chem. Technol*. **2018**, *12*, 305–309. https://doi.org/10.23939/chcht12.03.305
[30] Kuntyi, O. I.; Zozulya, G. I.; Shepida, M. V. Nanoscale Galvanic Replacement in Non-Aqueous Media: A Minireview. *Vopr. Khim. Khim. Tekhnol.* **2020**, *4*, 5–15. https://doi.org/10.32434/0321-4095-2020-131-4-5-15
[31] Zhong, K.; Huang, L.; Li, H.; Zhang, H.; Yang, R.; Arulmani S. R. B.; Liu, X.; Huang, L.; Yan, J. Enhanced Oxygen Reduction upon Ag/Fe co-Doped UiO-66-NH2-Derived Porous Carbon as Bacteriostatic Catalysts in Microbial Fuel Cells. *Carbon* **2021**, *183*, 62–75. https://doi.org/10.1016/j.carbon.2021.06.070
[32] Lüsi, M.; Erikson, H.; Piirsoo, H. M.; Aruvali, J.; Kikas, A.; Kisand, V.; Tamm, A.; Tammeveski, K. Oxygen Reduction Reaction on AgPd Nanocatalysts Prepared by Galvanic Exchange. *Appl. Surf. Sci*. **2023**, *636*, 157859. https://doi.org/10.1016/j.apsusc.2023.157859
[33] Jian, C.-c.; Zhang, J.; Ma, X. Cu–Ag Alloy for Engineering Properties and Applications Based on the LSPR of Metal Nanoparticles. *RSC Adv*. **2020**, *10*, 13277–13285. https://doi.org/10.1039/d0ra01474e

Received: July 09, 2025 / Revised: December 06, 2025 / Accepted: December 10, 2025

ЕЛЕКТРОВІДНОВЛЕННЯ КИСНЮ НА НАНОСТРУКТУРОВАНИХ СРІБНО-МІДНИХ КАТОДАХ

Анотація. *Запропоновано одержання каталітично активних катодів AgNPs/Cu із відновленням O_2 методом гальванічного заміщення срібла на мідь у розчинах $K[Ag(CN)_2]$. Показано, що утворені AgNPs розміром <50 нм рівномірно розподілені на мідній поверхні, а їхній вміст залежить від концентрації ціанокомплексу та тривалості процесу GR. Встановлено, що в широкому діапазоні концентрацій срібла (0,02–0,86 ат. %) на мідній поверхні катоди AgNPs/Cu проявляють на ~15 % вищу активність ORR, ніж срібні, та кращі показники Eonset (на ~0,02 V) і $E_{1/2}$ (на ~0,05 V). Результати тестування у лужних цинково-повітряних паливних елементах показали, що напруга розряду на основі AgNPs/Cu катодів конкурує із елементами на основі срібних катодів.*

Ключові слова: *ORR, біметалева поверхня, AgNPs/Cu катоди, гальванічне заміщення, $K[Ag(CN)_2]$ розчини.*